

Epitaxial Growth of Fe₃O₄ Films by Gas Flow Sputtering

Kiyoshi Ishii, Taro Satomi, and Akira Irino-uchi

Faculty of Engineering, Utsunomiya University, 7-1-2 Yoto, Utsunomiya 321-8585, Japan
 Fax: 81-28-689-6090, e-mail: ishiik@cc.utsunomiya-u.ac.jp

We studied epitaxial thin-film growth of magnetite (Fe₃O₄) by gas flow sputtering (GFS). GFS is a high-pressure sputtering (at about 100 Pa) and has characteristics between PVD and CVD; thus, the growth of high-quality magnetite films is expected. In this experiment, a pure Fe tube was used as the target and the oxygen gas was supplied in front of the substrate. Mirror-polished (100)MgO was used as the substrate because of the close lattice match. When the growth temperature was 350 °C and the flow rate of oxygen gas was 0.08 sccm, epitaxial growth of Fe₃O₄ was confirmed by observing sharp RHEED patterns. Such films had nearly the same values of magnetization and resistivity as those of bulk Fe₃O₄, and were observed to undergo a sharp Verwey transition at 120 K. It was also observed that heat treatment of MgO substrates at 1000 °C in O₂ decreased the temperature for the epitaxial growth from 350 °C to 300 °C.

Key words: magnetite film, Verwey transition, sputtering, sputtered film, gas flow sputtering

1. INTRODUCTION

The study of epitaxial thin-film growth of magnetite (Fe₃O₄) has attracted much attention. This is because thin films of magnetite and related iron oxides (such as γ -Fe₂O₃ and α -Fe₂O₃) are of importance for applications as planner devices in high-density magnetic recording and in microwave resonant circuits. Fe₃O₄ shows great promise for use as electrodes in spin-dependent transport devices. Epitaxial growth of Fe₃O₄ films on (100)MgO or (100)SrTiO₃ has been carried out by a variety of deposition techniques such as oxygen-plasma-assisted molecular beam epitaxy (MBE) [1] and pulsed laser evaporation [2]. Although sputtering has many advantages for a film growth processing, it has seldom been used for preparing epitaxial magnetite films, probably because of the existence of energetic particles in the process. In a sputtering process, many kinds of energetic particles impinge on the substrate; sputtered particles have a few eV, and reflected Ar and negative oxygen ions have much higher energies. Reflected Ar or O⁻ ions, which have high energies (over 100 eV), sometimes strike the substrate. Such particles may damage the film and are therefore a serious problem for the growth of films with good crystallinity. In order to prevent damage by energetic particles, sputtering is often carried out at a high pressure. High-energy particles lose their energy by collisions with Ar under high-pressure conditions where the mean free path is very short compared with the distance between the target and substrate. However, if the pressure is so high that the dissipation of their initial energy, i.e., thermalization, is completed near the target, the deposition rate decreases to a very small value.

Ishii developed a gas flow sputtering (GFS) method that enables high-rate deposition at a high pressure of about 100 Pa [3]. Under such high-pressure conditions, the thermalization of high-energy particles is completed in a very short distance [4]. GFS is based on a hollow cathode discharge and is schematically shown in Fig. 1. Hollow cathode discharge occurs in a hollow target, a tube or facing plates. Sputtered particles are transported by the directed Ar gas flow out of the hollow target

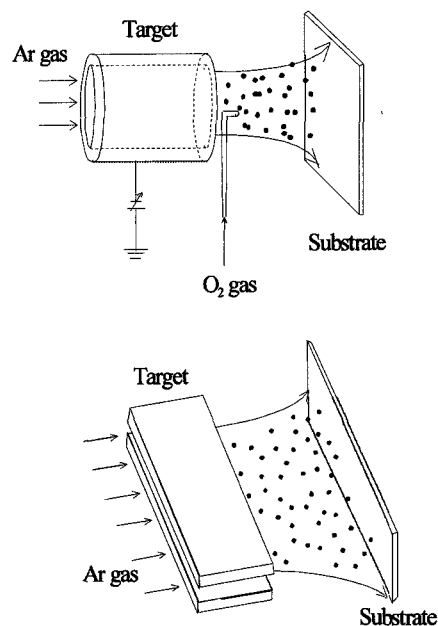


Fig. 1. Principle of gas flow sputtering.

towards the substrate. This leads to an effective deposition of low-energy (<0.1 eV) vapor. This mechanism also allows reactive sputtering with a high deposition rate. That is, a reactive gas (e.g., oxygen) can be added outside the hollow target. Due to Ar gas counter-flow, the reactive gas cannot penetrate the target. Thus, its reaction with the target surface is suppressed. Oxidation of the target surface, which is difficult to prevent in standard magnetron sputtering, results in a considerable decrease in deposition rate.

In this paper, we report the epitaxial growth of Fe₃O₄ thin films on MgO by GFS. The crystallinity, phase purity, and magnetic properties, including the Verwey transition of the films, are described and discussed.

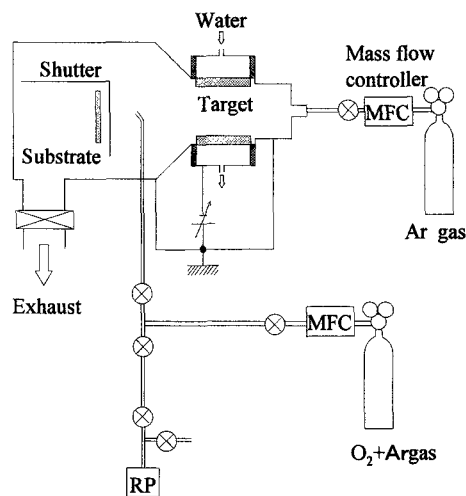


Fig. 2. Schematic diagram of gas flow sputtering system used in this work.

2. EXPERIMENTAL

Figure 2 shows a schematic diagram of the GFS apparatus used for the deposition of Fe_3O_4 films. The target was a 99.9% Fe tube with an internal diameter of 1.5 cm and length of 5 cm. As a sputtering gas, 99.9999% Ar gas was passed through the target. A mixture of O_2 (10%) and Ar (90%) was used for the addition of oxygen, and it was supplied into the Ar stream at the outlet of the target. The sputtering was carried out under the following conditions: Ar gas flow rate of 300 sccm, O_2 gas flow rates of 0 to 0.1 sccm, total pressure of 130 Pa, target-to-substrate separation of 10 cm, discharge power of 310 W, and deposition rate of about 3 nm/min. The film thickness was measured by a profilometer. The magnetite Fe_3O_4 films were grown on mirror-polished (100)MgO single crystals. Both cubic Fe_3O_4 and MgO have their oxygen atoms in a face-centered-lattice structure with a small mismatch of about -0.3%. Prior to the epitaxial growth of Fe_3O_4 films on MgO, we grew films on SiO_2 glass plates to determine the optimum O_2 gas flow rate for the formation of magnetite.

The film structure was characterized by conventional x-ray diffraction (XRD) and reflection high-energy electron diffraction (RHEED). Surface morphology was observed by atomic force microscopy (AFM). Resistivity measurements were carried out by the standard four-probe dc method, and magnetization data were obtained by the use of a vibrating sample magnetometer (VSM).

3. RESULTS AND DISCUSSION

First, we investigated the optimum O_2 flow rate at various growth temperatures for the growth of Fe_3O_4 , because the crystal structure of iron oxide films strongly depended on the O_2 flow rate F_o and the growth temperature T_s . Since the film structure is generally affected by the substrate, SiO_2 glass plates were used as the substrate. Figure 3 shows the ranges of formation of iron oxides as a function of F_o and T_s . The film thickness was fixed at 200 nm, and the phases were

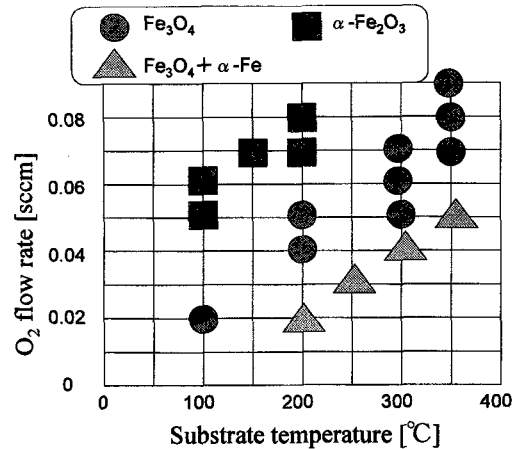


Fig. 3. Formation ranges of Fe, Fe_3O_4 , and $\alpha\text{-Fe}_2\text{O}_3$ as a function of substrate temperature and O_2 gas flow rate.

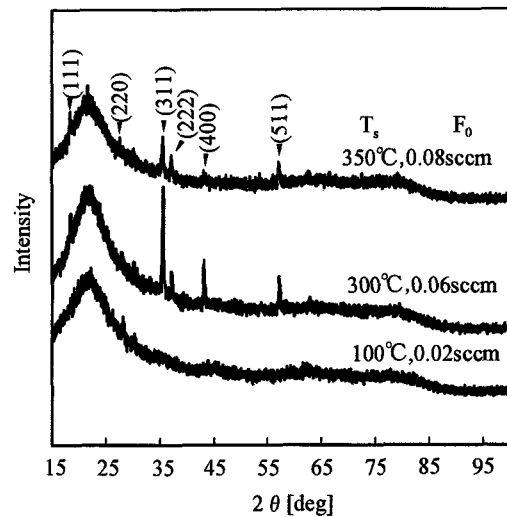
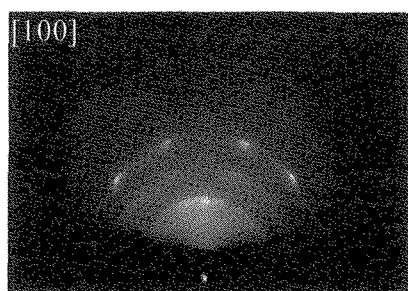


Fig. 4. XRD patterns of Fe_3O_4 grown on SiO_2 at various substrate temperatures T_s and O_2 gas flow rates F_o .

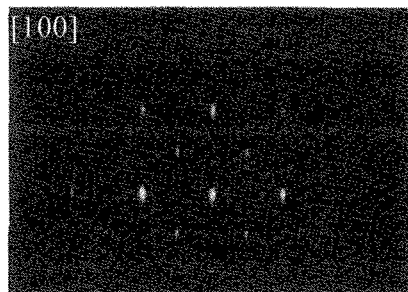
identified by XRD. In general, more-oxidized phases were deposited at low T_s and high F_o . The results presented in Fig. 3 show that the flow rate of O_2 gas is too small to be controlled for obtaining Fe_3O_4 films. However, it can be strictly controlled by a conventional mass flow controller if a diluted gas with Ar (e.g., 10% O_2 -90%Ar), which was used in this experiment, is used. Typical XRD patterns of single-phased Fe_3O_4 films grown at various temperatures are shown in Fig. 4. The reflection peaks in the XRD patterns became highest and narrowest at $T_s=300^\circ\text{C}$ and $F_o=0.06$ sccm. This temperature may be the most favorable for the growth of Fe_3O_4 crystallites. The values of magnetization and resistivity of the films shown in Fig. 4 are shown in Table I. The values of magnetization and resistivity of bulk Fe_3O_4 are 471 emu/cc [5] and $\sim 10^{-2} \Omega \cdot \text{cm}$ [6], respectively. The magnetization and the resistivity of films are nearly the same as those of bulk Fe_3O_4 . One

Table I Saturation magnetization M_s and resistivity ρ of Fe_3O_4 films grown on SiO_2 substrates.

T_s (°C)	F_0 (sccm)	M_s (emu/cc)	ρ ($\Omega \cdot \text{cm}$)
100	0.02	440	0.043
300	0.06	490	0.032
350	0.08	450	0.075



(a) $T_s = 300 \text{ }^\circ\text{C}$, $F_0 = 0.06 \text{ sccm}$

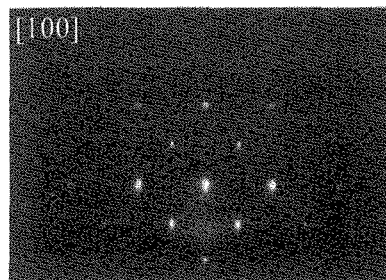


(b) $T_s = 350 \text{ }^\circ\text{C}$, $F_0 = 0.08 \text{ sccm}$

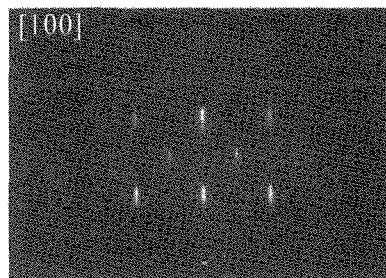
Fig. 5. RHEED patterns of Fe_3O_4 films grown on (100)MgO substrate.

possible cause of deviation is error in measurement of film thickness. Another possible cause is the existence of other phases in the film such as $\alpha\text{-Fe}$ or $\alpha\text{-Fe}_2\text{O}_3$. However, it is difficult to identify all of the produced phases from the XRD patterns and the properties.

Next, we deposited Fe_3O_4 films on (100)MgO and investigated the epitaxial growth. The RHEED patterns of 200-nm-thick Fe_3O_4 films grown at 300 °C and 350 °C are shown in Fig. 5. When T_s was set at 300 °C and 350 °C, F_0 was set at 0.06 sccm and 0.08 sccm, respectively; these conditions were the optimum O_2 flow rate for SiO_2 substrates. As can be seen in Fig. 5, a spot pattern was observed at temperatures above 350 °C, and Debye rings were observed at lower temperatures. It was judged from the RHEED patterns and their azimuth dependence that Fe_3O_4 films were epitaxially grown at



(a) $T_s = 300 \text{ }^\circ\text{C}$, $F_0 = 0.06 \text{ sccm}$



(b) $T_s = 350 \text{ }^\circ\text{C}$, $F_0 = 0.08 \text{ sccm}$

Fig. 6. RHEED patterns of Fe_3O_4 films grown on (100)MgO substrate heat-treated at 1000 °C for 1 h in 1-atm O_2 prior to the deposition.

temperatures above 350 °C with the (100) plane parallel to the (100)MgO. Although crystal growth was promoted more at $T_s=300 \text{ }^\circ\text{C}$ than at $T_s=350 \text{ }^\circ\text{C}$ on SiO_2 substrates, the epitaxial growth occurred at $T_s=350 \text{ }^\circ\text{C}$ on MgO. This shows that the initial layer needs a higher temperature to grow hetero-epitaxially on MgO. We also investigated the influence of F_0 on epitaxial growth. At $F_0=0.07 \text{ sccm}$ and $T_s=350 \text{ }^\circ\text{C}$, nearly the same RHEED pattern was observed. On the other hand, when F_0 was increased to 0.09 sccm at $T_s=350 \text{ }^\circ\text{C}$, Debye rings from the Fe_3O_4 phase were mixed in the spot pattern, indicating poor epitaxi. Since the Debye rings were not from a more-oxidized $\alpha\text{-Fe}_2\text{O}_3$ phase but from the Fe_3O_4 phase, this result reveals that the growth of a crystal, which is affected by O_2 partial pressure, is also important for the epitaxial growth. It was also observed that the reflection peaks in the XRD pattern became small and wide with increase in F_0 from 0.08 sccm to 0.09 sccm for growth on SiO_2 .

On the other hand, it was observed that heat treatment of an MgO substrate resulted in a considerable decrease in the epitaxial growth temperature. The (100)MgO was heated at 1000 °C for 1 hour in 1-atm O_2 prior to setting in the deposition chamber. As a result, epitaxial growth was observed at 300 °C. The RHEED patterns of Fe_3O_4 films grown on heat-treated MgO at $T_s=300 \text{ }^\circ\text{C}$ and 350 °C are shown in Fig. 6. Both of them are patterns from a single crystal magnetite. When the MgO substrate was not heat-treated, polycrystalline films were obtained at 300 °C (see Fig. 5). This suggests that the heat treatment improves the surface structure of MgO in atomic scale and results in a

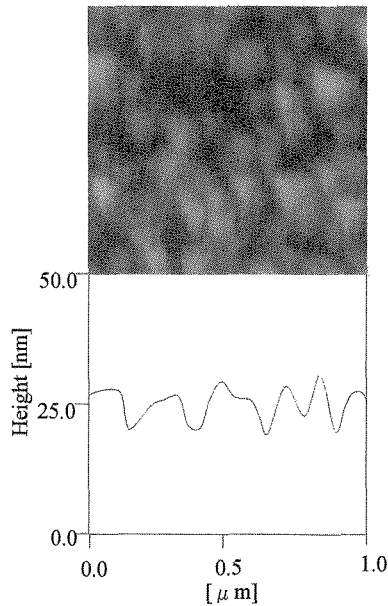


Fig. 7. AFM image of Fe_3O_4 film shown in Fig. 6(b).

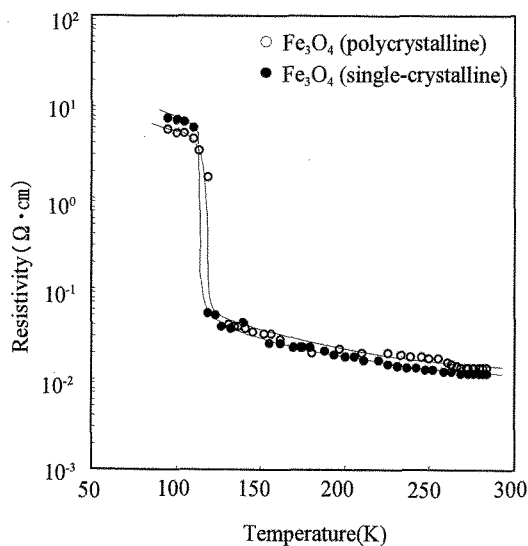


Fig. 8. The resistivity as a function of temperature for polycrystalline Fe_3O_4 film shown in Fig. 5(a) and single-crystalline Fe_3O_4 film shown in Fig. 6(b).

decrease in epitaxial growth temperature. When SiO_2 was used as the substrate, polycrystalline films were grown and the growth of crystal grains was promoted the most at 300 °C. However, in the case of MgO substrate, the diffraction spots of a film grown at 350 °C become sharper than those of a film grown at 300 °C, as shown in Fig. 6. A film grown at $T_s=350$ °C must have better crystallinity and a flatter surface.

Figure 7 shows an AFM image of an Fe_3O_4 film grown on heat-treated MgO at 350 °C. Although the microstructure of each grain could not be observed, the film surface was considerably flat, with roughness of

about 11 nm. A smoother surface could be obtained by optimizing the preparation conditions, including growth rate and treatment of the substrate surface.

At a temperature around 120 K, Fe_3O_4 undergoes the so-called Verwey transition in which the conductivity decreases by a factor of ~ 100 and a second-order structural transition takes place. The sharpness and temperature of the Verwey transition are good indications of crystallinity and phase purity of Fe_3O_4 films [7]. Thus, we investigated the temperature dependence of resistivity for Fe_3O_4 films obtained on (100)MgO. Figure 8 shows the results for a polycrystalline film (shown in Fig. 5 (a)) and a single crystal film (shown in Fig. 6 (b)). For both films, a very sharp Verwey transition is seen at about 120 K, indicating that these films are well-crystallized and single-phased magnetite films [1][2].

In GFS, the glow plasma penetrates from the hollow target and exists around the substrate. In this experiment, we did not measure the density of plasma. However, it generally decreases rapidly with increase in the target-to-substrate separation, and it is assumed to be very low in this case. Consequently, film growth similar to that of CVD occurred. The growth of magnetite films with good crystallinity and high phase quality is attributed to the low energy process like CVD.

4. CONCLUSION

Iron oxide films were reactively sputtered by the GFS method, and the utility of this method for controlling the film phase was confirmed. And suitable conditions for preparing single-phased Fe_3O_4 films and also (100)-oriented epitaxial Fe_3O_4 films were determined. The Verwey transition was observed for polycrystalline and single-crystalline Fe_3O_4 films. The observation of the Verwey transition indicates that Fe_3O_4 films obtained by GFS have well-crystallized and stoichiometric characters. By optimizing the preparation conditions, including deposition rate and substrate processing, it will be possible to obtain high-quality magnetite films with very smooth surfaces in atomic scale by GFS.

REFERENCES

- [1] J. F. Anderson, M. Kuhn, U. Diebold, K. Shaw, P. Stoyanov, and D. Lind, *Phys. Rev. B* **56**, 9902 (1997).
- [2] X. W. Li, A. Gupta, G. Xiao, and G. Q. Gong, *J. Appl. Phys.*, **83**, 7049 (1998).
- [3] K. Ishii, *J. Vac. Sci. Technol. A* **7**, 256 (1989).
- [4] R. E. Somekh, *J. Vac. Sci. Technol. A* **2**, 1285 (1984).
- [5] *Magnetic and Other Properties of Oxides and Related Compounds*, edited by K. -H. Hellwege and A. M. Hellwege, *Londolt Börnstein, New Series, Group III, Vol.4, pt. B* (Springer-Verlag, Berlin, 1970).
- [6] T. Fujii, M. Takano, R. Katano, Y. Bando, and Y. Isozumi, *J. Appl. Phys.*, **66**, 3168 (1989).
- [7] J. J. Kerbs, D. S. Lind, and S. D. Berry, *J. Appl. Phys.*, **73**, 6457 (1993).

(Received February 5, 2003; Accepted June 30, 2003)